Synthesis of a Labeled RGD−Lipid, Its Incorporation into Liposomal Nanoparticles, and Their Trafficking in Cultured Endothelial Cells

Sonya Cressman,* Ian Dobson, Justin B. Lee, Yuen Yi C. Tam, and Pieter R. Cullis

Department of Biochemistry and Molecular Biology, University of British Columbia, Life Sciences Centre, 2350 Health Sciences Mall, Vancouver, Canada V6T 1Z3. Received January 29, 2009; Revised Manuscript Received May 25, 2009

The use of targeting ligands to enhance the delivery of liposomal nanoparticles (LNs) has moved slowly toward clinical application. This relative lack of clinical progression is further complicated by the existence of conflicting *in vivo* results in the literature. In this work, we describe new formulations of LNs that are targeted with an arginine-glycine-aspartic acid-containing peptide, cRGDfK, conjugated to the lipid distearoyl phosphatidylethanolamine (DSPE). These formulations may be able to circumvent some of the challenges encountered during the development of targeted-LNs. Of the constructs studied, a fluorescently labeled peptide−lipid conjugate was incorporated into LNs with high yield and accuracy. It is shown that the resulting targeted-LNs bind to human umbilical vein endothelial cells (HUVECs) with increasing avidity as the amount of peptide displayed on the LN surface increases. We specifically demonstrate the ability of targeted-LNs loaded with doxorubicin and incubated with HUVECs to deliver the drug to the cytosol. The cell does not internalize nontargeted LNs, supporting the notion that the RGD motif is associated with internalization of the targeted LN.

INTRODUCTION

In order for liposomal nanoparticles (LNs) to reach cancer cells, they must survive for prolonged amounts of time in the circulatory system (*1*). The addition of a targeting ligand to the surface of an LN is thought to increase the accumulation of the LN by increasing its affinity for a specific target on the surface of diseased cells. Vascular targeting, as opposed to targeting tumor cells themselves, offers the additional advantage of being a relatively general therapy for the treatment of solid tumors, given that all tumors require neovasculature in order to survive (*2*). Cells that make up the tumor vasculature (mainly endothelial cells) are also ideal anticancer targets, as they are not expected to generate drug-resistant variants. The methods described here utilize an arginine-glycine-aspartic acid (RGD) peptide to aid in targeting LNs to endothelial cells containing the molecular target, the $\alpha_v\beta_3$ integrins.

RGD-conjugated drugs have been investigated for their ability to bind to the $\alpha_v\beta_3$ integrins for over fifteen years (*3*). In the late 1990s, medicinal chemists pinpointed a highly selective RGD peptide, which is now an antiangiogenesis drug candidate in phase II clinical trials (*4, 5*). Since the early 2000s, RGD-targeted drugs (*6*), imaging agents (*7*−*9*), antibodies (*10*), and LNs (*11*−*13*) have used cyclic RGD-containing peptides to guide cargo to the tumor-associated vasculature *in vivo*. The timely rate of clinical progression of RGD peptides without cargo and well-defined RGD-imaging agents indicates that RGD-based drugs may be promising new therapies of the future (*9, 14*). RGD-targeted LNs, on the other hand, do not show a sufficient rate of clinical progression.

Targeted-LNs, in general, have held the interest of pharmaceutical innovators since the 1980s (*15*−*17*). RGD-targeted LNs are the most structurally simplified of the known targeting ligands. Despite the relative simplicity of using short peptides as targeting ligands, studies on RGD-LNs tend not to describe the physical and chemical properties of the final product (*11*−*13*). The current theories of the *in vivo* behavior of RGD-LNs are also divergent. While some reports indicate that RGD-LNs share similar *in vivo* circulation lifetimes to nontargeted LNs (*11, 12*), others report the accelerated clearance of RGD-LNs (*13*).

Perhaps the greatest accomplishment toward clinical advancement of targeted-LNs is the first report on the preclinical manufacture of a protein−polymer−lipid micelle, which focuses solely on characterization (*18, 19*). For clinical progression, targeted-LN drug candidates will be required to demonstrate compliance with the regulatory codes of good manufacturing practice. We propose that, in order to move RGD-LN technology toward the clinic, a step backward is necessary to understand what is happening in targeted-LN formulation.

This study focuses on the construction of well-defined RGD-LNs. The RGD-lipid construct with the best formulation properties was purified and qualitatively assessed. A fluorescent label, methoxycoumarin (MCA), was used to track the amount of the purified RGD-lipid construct that is incorporated into an RGD-LN by one of two published methods: either the postinsertion method (*20*) or by classic liposome formulation methods (*21*). Our results also describe the optimal mole fraction of RGD-lipid that enables high target binding and drug delivery via defined RGD-LNs to the cytosol of $\alpha_v\beta_3$-expressing cells.

EXPERIMENTAL PROCEDURES

Materials and Reagents. Unless specified, all reagents were of reagent-grade quality or better. Reversed-phase HPLC (RP-HPLC) was performed using gradients of aqueous acetonitrile containing 0.1% trifluoroacetic acid (TFA) (aqACN) applied to C18 columns. Analytical gradients were run using a 150 mm × 4.6 mm column with a flow rate of 1 mL per minute. Peptides were purified on a preparative scale with a 250 mm × 22 mm column and a flow rate of 10 mL per minute.

Peptide Synthesis. Dimethylformamide (DMF) was the main solvent used for peptide synthesis, unless otherwise specified. The linear sequence D(t-Bu)fK(Z)R(Pbf)G (The RGD-containing peptide) was synthesized by FMOC-based solid-phase peptide synthesis as described previously (*22*). Briefly, peptides were assembled on 0.5 mmol of 2-chlorotrityl resin using 1.3 mol equiv (to carboxylic acid) of the following activating agents:

* E-mail: scressman@bccrc.ca. Lab Phone: (604)-822-4955. Office Phone: (604)-822-6263. Fax: (604)-822-4843.

10.1021/bc900041f CCC: $40.75
Published on Web 06/17/2009

O-benzotriazole-*N*,*N*,*N*′,*N*′-tetramethyl-uronium hexafluorophosphate (HBTU) and *N*-hydroxybenzotriazole (HOBT). Peptides were activated *in situ* with triethylamine (TEA), then coupled to the resin for at least 1 h. FMOC removal steps were performed upon each amino acid addition by soaking the resin in a solution of 20% piperidine in DMF for 5 min and repeated once. Between each step, the resin was washed with a constant flow of DMF for at least 1 min. Linear peptides were cleaved in 0.1% TFA in dichloromethane (DCM) with 2.5% triisopropyl silane (TIS) and H_2O (v/v). The crude peptide was analyzed by RP-HPLC with a linear gradient of 30−90% aqACN over 30 min (retention time = 16.3 min) and by electrospray mass spectrometry (ESI-MS).

Lyophilized linear peptides were cyclized at 0.5 mM in DMF using benzotriazol-1-yl-oxytripyrrolidiniophosphonium hexafluorophosphate (PyBop) and HOBT to produce cR(Pbf)GD(t-Bu)fK(Z). Cyclization yields were typically greater than 95% and occurred within 30 min, as indicated by RP-HPLC, with a retention time of 19.5 min on the same gradient as the linear peptide and a difference of −18 in the observed molecular weight by ESI-MS. ^{1}H NMR NOE assignments for all α-amide bonds confirmed a head-to-tail cyclic compound.

The benzyl group on the lysine side chain was removed by hydrogenation using a palladium/carbon catalyst. The amine-functionalized peptide, cR(Pbf)GD(t-Bu)K (100 mM in DMF), was modified with 10 mol equiv of succinic anhydride to produce cR(Pbf)GD(t-Bu)fK(succ). The reaction mixture was purified with an RP-HPLC gradient of 10−60% aqACN over 1 h. A 95% pure product eluting after 40 min was characterized both by ESI-MS (MW = 1011.47 ± 1) and by analytical RP-HPLC using a 30−90% aqACN gradient, a product of >95% purity was obtained, with a retention time of 12.1 min.

cR(Pbf)GD(t-Bu)fK-PEG$_2$-K(MCA)-PEG$_2$-COOH Synthesis. Four strategies to synthesize RGD-lipids were investigated (see Supporting Information for a summary of these approaches). We focus on the RGD-lipid construct, which displayed the best characteristics for producing a targeted LN. The synthesis of this chosen construct is described herein.

The spacer−peptide conjugate was assembled as follows: 0.112 mmol 2-chlorotrityl resin was loaded with 2.5 mol equiv of *O*-(*N*-Fmoc-3-aminopropyl)-*O*′-(*N*-diglycoyl-3-aminopropyl)-di(ethylene glycol) (Fmoc-NH-PEG$_2$-COOH) over the course of 3 h, under nitrogen gas with gentle stirring. FMOC was removed by soaking the resin in a solution of 20% piperidine in DMF for 5 min, and repeated once. Ninhydrin assays were used to monitor the success of solid-phase synthesis reactions. 2.5 mol equiv of Fmoc-Lys-(MCA)-OH were then coupled to the free amine using 1.2 mol equiv to carboxylic acid of HOBT, HBTU, and TEA for 1 h, then subsequently, 5 mol equiv of the second Fmoc-NH-PEG$_2$-COOH unit was incorporated over 3 h using 1.2 mol equiv to carboxylic acid of PyBop, HOBT, and TEA. Trial cleavages (performed in a solution of 0.1% TFA in DCM, 2.5% H_2O, 2.5% TIS (v/v)) proved to be more reliable than ninhydrin assays for monitoring the success of each coupling reaction from this point on, presumably due to the shielding effect of PEG. The product (after step d of Figure 1) was retained for 21 min by an analytical RP-HPLC gradient 0−85% aqACN over 30 min. Successful Fmoc removal resulted in a shift in retention time to 14.5 min, using the same gradient. 1.2 mol equiv (to amine) of the cyclic peptide, cR(Pbf)GD(t-Bu)fK(succ), was coupled overnight to the spacer under nitrogen gas using 1.2 mol equiv of PyBop and HOBT and TEA to acid. The product cR(Pbf)GD(t-Bu)fK-PEG$_2$-K(MCA)-PEG$_2$-COOH was purified directly by preparative RP-HPLC (0−85% aqACN) eluting after 40 min.

The dry yield of the peptide−spacer construct was 80 mg. The product was clearly resolved by TLC (chloroform ($CHCl_3$)/methanol (MeOH), 8.8/2.2), R_f = 0.18, and purified to >95% purity as indicated by analytical RP-HPLC (0−85% aqACN). The correct product was validated by ESI-MS.

Synthesis of cRGDfK-PEG$_2$-K(MCA)-PEG$_2$-DSPE. The peptide−spacer construct was conjugated with the lipid anchor, DSPE in a solution. The purified and lyophilized peptide−PEG constructs were dissolved in 2 mL DCM and activated with 5 mol equiv of *N*-hydroxysuccinimide and diisopropylcarbodiimide. The active ester formed within 30 min, and 3.5 mol equiv to acid of distearylphosphatidyl ethanolamine (DSPE) was dissolved in 1 mL $CHCl_3$ at 60 °C. The activated ester was then added to the lipid with 1.2 mol equiv (to ester) of TEA. The reaction occurred within 1 h at 60 °C, and the resulting product was purified on 100 g of silica gel, mobile phase MeOH/$CHCl_3$. The product, cR(Pbf)GD(t-Bu)fK-PEG$_2$-K(MCA)-PEG$_2$-DSPE, eluted between 30−50% methanol in $CHCl_3$ and was identified by TLC ($CHCl_3$/MeOH 8.8/2.2, R_f = 0.74).

The compound was concentrated and redissolved in 95% aqueous TFA to deprotect the arginine and aspartic acid side chains. The product formed within 2 h. TFA was removed by gentle evaporation under a stream of nitrogen, precipitated into ice-cold diethyl ether, centrifuged, rinsed with diethyl ether, and centrifuged again. A yield of 40.8 mg of cRGDfK-SUCC-PEG$_2$(MCA)-PEG$_2$-DSPE (herein, referred to as the RGD-lipid) resulted. The ESI-MS MW for RGD-lipid was 2415.5 ± 1 (predicted MW = 2414.89). Purity of RGD-lipid was confirmed by TLC detected with iodine and UV (MeOH/EtOH/H_2O/TEA (6/3/1/1) R_f = 0.25. Excitation (325 nm) and emission (389 nm) spectra were collected for the construct between 280 and 500 nm using a fluorometer.

Formation of Liposomal Nanoparticles. Dry lipids were dissolved in warm $CHCl_3$ at 60 °C. The solvent was removed under a stream of nitrogen gas to form a thin film, and residual solvent was removed by lyophilization. For empty vesicles, the thin film was hydrated in 100 mM HEPES buffer containing 144 mM NaCl, pH 7.5 (HBS), warmed to 60 °C. The resulting multilamellar vesicles were extruded through two polycarbonate filters with a 100 nm pore size. The vesicles were extruded ten times using an extruder, to form unilamellar LNs.

The mean diameter of the LNs was characterized by dynamic light scattering (DLS) using a Nicomp 370 particle sizer for size distribution analysis. LNs were further characterized by a phosphate assay using the method of Fiske and Subbarow, and by fluorescence emission at 590 nm, upon excitation at 530 nm. RGD-lipids were then incorporated into LNs by one of two methods, either the "post-insertion method" or the "formulation method".

Post-Insertion Method of Incorporating cRGDfK-PEG$_2$-K(MCA)-PEG$_2$-DSPE into Preformed LNs. The post-insertion method of incorporating a ligand-conjugated lipid into preformed LNs has been described previously (*20*). Our LNs were composed of the following lipids: 54 mol % distearylphosphatidylcholine (DSPC)/45 mol % cholesterol (Chol)/0.5 mol % Rhodamine-labeled phosphatidylethanolamine (Rhod:PE). After LNs were prepared as described in the above section, the required amount of RGD-lipid needed to make 1 mol % (RGD-lipid) was prepared as a micelle solution in HBS, at 65 °C. The LNs and RGD-lipid micelles were coincubated together at 65 °C for 2 h. The mixture was purified on a 40 mL Sephadex G50 column. Incorporation of the RGD-lipid into the LN was measured by MCA emission at 389 nm, following excitation at 325 nm in HBS containing 1% Tween 20 and compared against a standard curve made with known amounts of the RGD-lipid.

Formulation Method of Incorporating RGD-Lipids Into LNs. Empty RGD-LNs were also made using the "formulation method". We chose this method to manufacture RGD-LNs for studies on the drug retention characteristics of the LNs and for

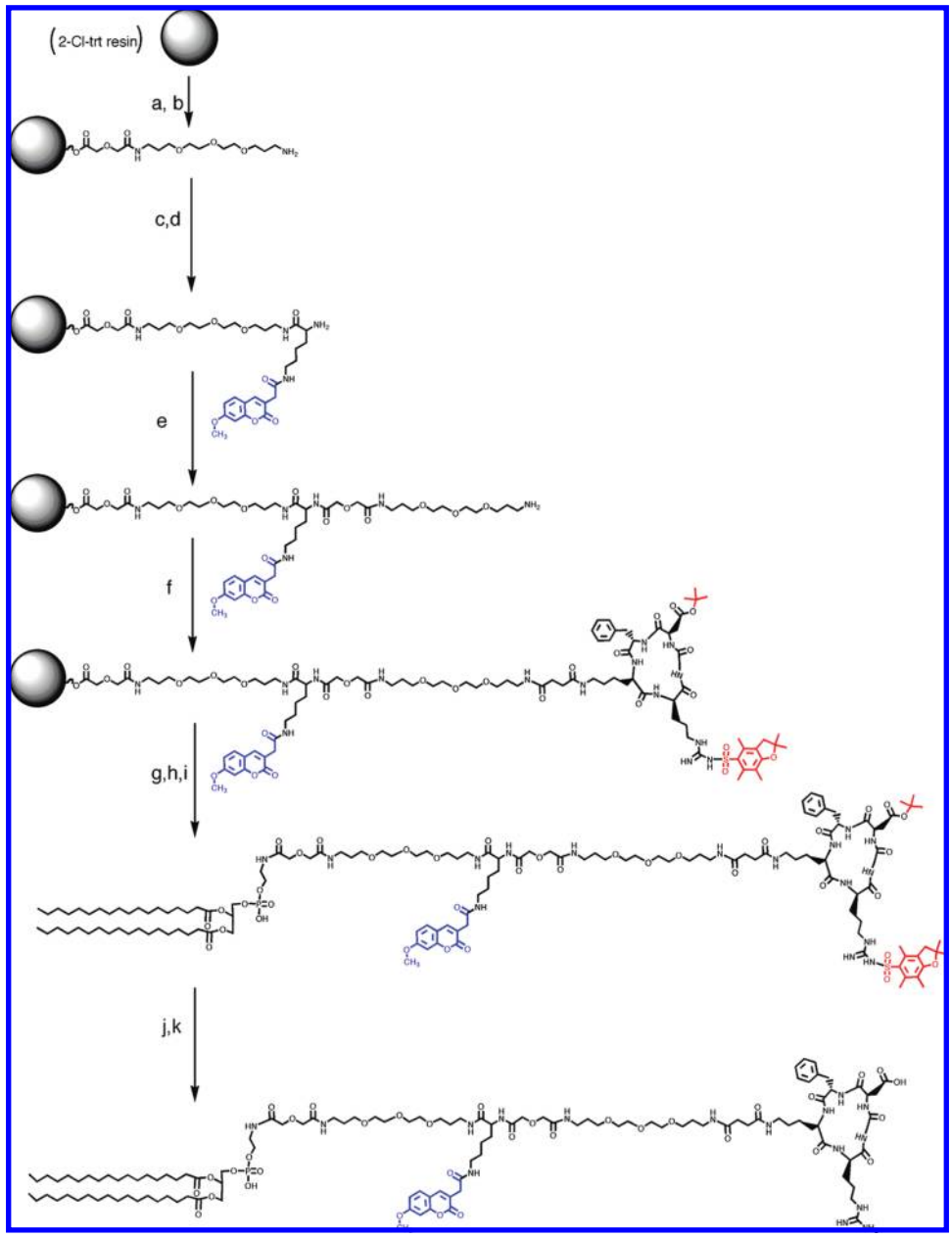

Figure 1. Synthesis of cRGDfK-PEG_2-K(MCA)-PEG_2-DSPE. (a) FMOC-PEG_2-OH, 3 h; (b) 20% piperidine in DMF; (c) Fmoc-Lys(MCA)-OH, HBTU/HOBT; (D) 20% piperidine in DMF; (e) FMOC-PEG_2-OH, PyBop/HOBT, 6 h; (f) cR(Pbf)GD(tBu)fK-succinic acid, PyBop/HOBT, 12 h; (g) 0.1% TFA, 1% TIS, 3.9% H_2O, 95% DCM; (h) RP-HPLC; (i) DSPE, PyBOP/HOBT, $CHCl_3$, 60 °C; (j) silica gel chromatography; (k) 95% TFA, 5% DCM, silica gel chromatography.

all cell-based assays. We varied the amount of RGD per LN by increasing the mol % of the RGD-lipid added before the LNs were formed. The series of RGD-LNs containing different amounts of RGD were formulated as follows: 0.5 mol % RGD-LN was made by incorporating: 54 mol % distearylphosphatidylcholine (DSPC)/45 mol % cholesterol (Chol)/0.5 mol % Rhodamine-labeled phosphatidylethanolamine (Rhod:PE)/0.5 mol % RGD-lipid (i.e., 54:45:0.5:0.5 mol:mol), 1 mol % RGD-LN (53.5:45:0.5:1) mol:mol), 2.5 mol % (52:45:0.5:2.5 mol:mol), and 5 mol % (49.5:45:0.5:5 mol:mol). Nontargeted LNs were formulated as (54.5:45:0.5:0 mol:mol). For drug retention and biological assays on intracellular delivery, 0.5 mol % RGD-LNs were used.

The amount of surface-exposed RGD-lipid per liposome was estimated under the assumption that one LN contains approximately 148 641 lipids (based on the average diameter of the particle being 116 nm, and the average surface area of a lipid headgroup as 0.5 nm^2). For this diameter, the proportion of those lipids residing in the outer leaflet is approximately 57% of the total lipid composition.

Comparison of the Post-Isertion and Formulation Methods for RGD-LN Formation. The postinsertion and formulation methods were compared with regard to their ability to incorporate RGD-lipid into LNs. In order to quantify the amount of the RGD-lipid that was incorporated into the LN by either method, the fluorescence emission and excitation spectra were obtained for the RGD-lipid (Figure 2). The amount of the targeting ligand that was incorporated by either the post-insertion or the formulation method was subsequently measured by fluorometry. Fluorometric measurements were conducted in the presence of 1% Tween 20 in order to disrupt the LN structure. A linear increase in the fluorescence signal corresponded to increasing amounts of RGD-LNs;therefore, a standard curve was established from known amounts of the RGD-lipid in the presence of nontargeted LNs. The amount of RGD-lipid present

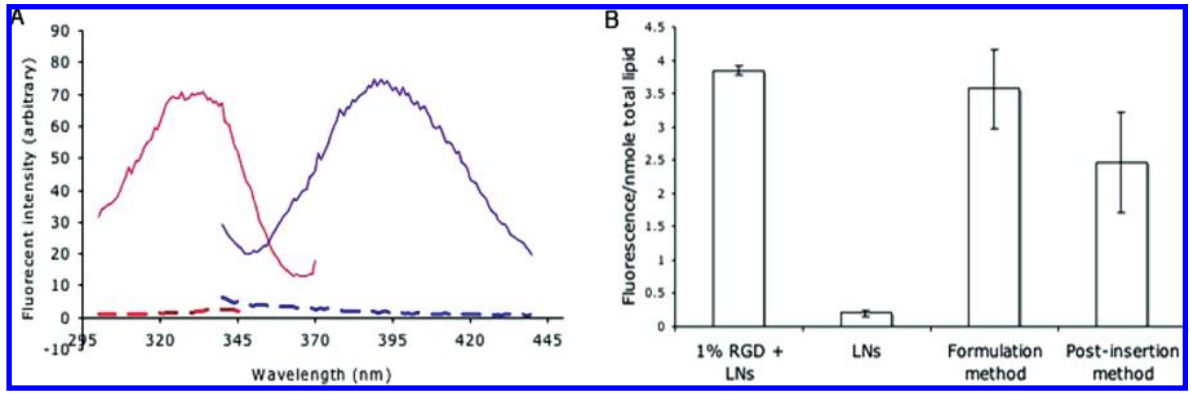

Figure 2. () Excitation (red) and emission (blue) spectra obtained for RGD-LNs with the RGD-lipid embedded in the bilayer. The spectrum for nontargeted LNs is shown by dashed lines. () Fluorescence measurements of the relative amounts of the RGD-lipid in RGD-LNs made by either the formulation method or the postinsertion method. The starting concentrationsof RGD-lipid (1 mol % of the total lipid concentration) plus nontargeted LNs represents the maximum possible RGD-lipid incorporation that was used before the RGD-lipid was incorporated into an LN.

in LNs made by the two different techniques was calculated as shown in Figure 2B.

HPTS Loading. In order to track intracellular delivery of LN contents, the pH-sensitive probe, 8-hydroxypyrene-1,3,6-trisulfonic acid (HPTS),was loaded into nontargeted LN and 0.5% RGD-LN (i.e., HPTS/N (55:45:0:0 mol:mol) and HPTS/GD-LN (54.5:45:0:0.5 mol:mol)). LNs were hydrated in 10 mL of HBS containing 40 mM HPTS, extruded,and dialyzed three times for 12 h against 4 L HBS. The resulting HPTS-LNs were characterized by DLS, phosphorus content,and HPTS fluorescence emission at 450 nm following excitation at 395 nm. The contribution from the MCA group of the RGD-lipid was examined and found to be negligible at this wavelength of detection.

Doxorubicin Loading ito the Interior of LNs. Doxorubicin was loaded into preformed nontargeted LNs and 0.5% RGD-LNs using the ammonium sulfate method described previously (*23*). Briefly, LN lipids were dried to a thin film,then hydrated in 10 mL of 300 mM ammonium sulfate, extruded,and dialyzed twice over 12 h against 150 mM NaCl. Phosphate assays were conducted to determine the amount of doxorubicin required to achieve a drug-to-lipid ratio of 0.2 (mol:mol). The appropriate amount of doxorubicin was dissolved in 1 mL of 150 mM NaCl, and the appropriate volume was delivered to each solution of LNs. Doxorubicin and LNs were coincubated at 55 °C for 1 h to load the drug, and then the free drug was removed by size exclusion chromatography, with a 40 mL Sephadex G50 column, equilibrated in 150 mM NaCl. Doxorubicin-encapsulated LNs (Dox:LNs) eluted within the first 10 mL fraction, and free doxorubicin eluted over the following 15 mL fractions. The size of the resulting particles was estimated by dynamic light scattering and assayed for phosphate content. The amount of encapsulated material was determined by RP-HPLC, using a standard curve made from the integrated peak area of doxorubicin's 280 nm UV absorbance. Free doxorubicin elutes on a 0−85% aqACN gradient at 15.8 min.

Doxorubicin Leakage Assay. The amount of doxorubicin that was retained in the LNs was measured over 24 h by the following doxorubicin leakage assay. Doxorubicin-loaded 0.5% RGD-LN and nontargeted LN (i.e., Dox:RGD-LN and Dox:LN), corresponding to an assay-confirmed concentration of 0.25 mM free doxorubicin, were incubated with 30% (v/v) FBS, total volume 1.5 mL, at 37 °C over 24 h. During this time, 100 μL was removed in duplicate at 0 min, 30 min, 1 h, 2 h, 5 h, and 24 h time points. The sample was applied to a spin column composed of 750 μL Sephadex G50 and centrifuged at 100 rpm for 1 min. One milliliter of 10% Triton X-100 (v/v) in 150 mM NaCl was added to the eluent in order to release the LN-entrapped doxorubicin. Doxorubicin content was subsequently assayed using the fluorescence emission of doxorubicin at 590 nm when compared to a standard curve made from free doxorubicin in 10% Triton X-100, 150 mM NaCl.

Cell Culture and LN Binding Assays. HUVEC cells, media, and supplements were obtained from Cascade Biologics (Portland, OR). M21 and M21L melanoma cell lines were obtained from Dr. D. Cheresh and were maintained in Dulbecco's Modified Eagle Medium supplemented with 10% fetal bovine serum (FBS). Rhodamine-labeled LNs varying in their RGD content (i.e., containing between 0 and 5 mol % of the targeting lipid) were added to cells to construct binding isotherms (Figure 3). LNs were adjusted to have equivalent phosphate content by dilution with HBS, then added to cells at concentrations between 0 and 4 mM (total lipid content). The final volume was adjusted to 500 μL with 5% FBS in PBS (PBS/FBS). Cells were incubated with LNs for 1 h at either 4 or 37 °C. After incubation, unbound LNs were removed with 5 mL of PBS/FBS, followed by centrifugation at 1100 rpm for 5 min, repeated twice. Unfixed cells were kept on ice and immediately analyzed by flow cytometry using a BD LSR II flow cytometer equipped with an air-cooled argon laser. Light scattering and fluorescence channels were set to a logarithmic scale and 10 000 events were collected per sample. Data were analyzed using *Flow Joe* (version 4.5.9, Stanford, CA). Electronic gates were established using unstained live cells based on their ability to exclude the uptake of propidium iodide. The mean fluorescence intensity was plotted versus the concentration of LN. Statistical analyses were conducted using *GraphPad Instat*, version 3.0. A Tukey-Kramer multiple comparisons test was used, with n values of 3, representing triplicate data points. P values greater than 0.05 were considered insignificant.

Cellular HPTS Uptake. HPTS:LNs and HPTS:RGD-LNs were added to cells and incubated at 37 °C for 0, 5, 15, 30, and 90 min time points. The cells were rinsed and assayed for cell-associated HPTS fluorescence by flow cytometry. At neutral pH, HPTS fluoresces at 519 nm when excited by light at 488 nm. Acidification of the vesicles (pH ~6.5−7) was monitored by detecting fluorescence emission at 455 nm following excitation at 405 nm. The background binding shown by nontargeted HPTS-containing LNs was low, and this measurement was subtracted from the fluorescence signals produced by RGD-LNs.

Doxorubicin Uptake into Cells as Determined by Flow Cytometry. 80 μM of doxorubicin (either encapsulated within the LN or as the free drug) was added to each aliquot of M21, M21L or HUVEC cells. The mixture was incubated for 90 min

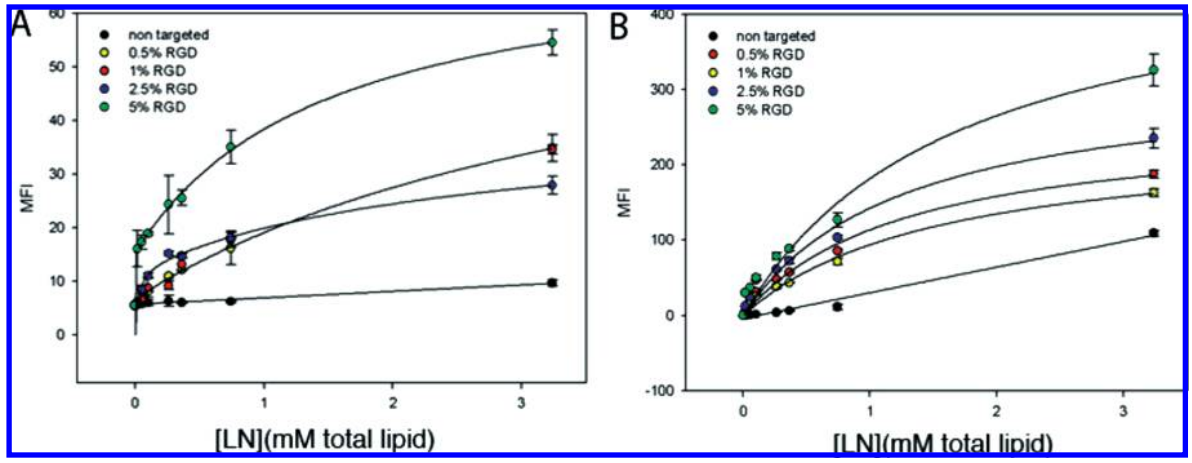

Figure 3. (A) Saturation curves describing the binding of LN to HUVEC following a 1 h incubation at 4 °C (endocytosis is prohibited at low temperatures). The LNs contain between 0 and 5 mol % RGD-lipid. (B) The same binding experiment conducted at endocytosis permissive temperatures (37 °C).

at 37 °C, then assayed for cell-associated doxorubicin fluorescence by flow cytometry as described in the above section.

LN Uptake into Cells as Observed by Fluorescence Microscopy. HUVEC cells were grown to confluence on four chambered glass slides (BD, Franklin Lakes, NJ). Cells were rinsed three times with PBS/FBS. 0.265 mM of doxorubicin was added for a final volume of 125 μL. For HPTS uptake, 1.36 mM (total lipid concentration) was added with a final volume of 200 μL. LNs or free drug were added to the cells; the mixture was incubated at 37 °C for 30 min, rinsed twice with PBS/FBS, and the cells were then fixed with 3.5% paraformaldehyde in PBS for 15 min and rinsed once again with PBS/FBS. Immediately before imaging, chambers were removed and slides were prepared using Vectashield mounting media (Vector Laboratories, Burlingame, USA) containing the blue nuclear stain, 4′,6-diamidino-2-phenylindole (DAPI). Images were captured using a Zeiss Axiovert 200 fluorescence microscope equipped with a Retiga 200R camera. Those acquired under a bright field used a 0.3 s exposure time and in the fluorescence field were acquired using three fluorescence filters with the following exposure times: red 3.5 s, green 5.5 s, DAPI 0.5 s.

RESULTS

Synthesis of Targeting Lipids. We synthesized the RGD-lipid, cRGDfK-SUCC-PEG$_2$(MCA)-PEG$_2$-DSPE using a straightforward solid-phase synthesis procedure, as shown in Figure 1. The final product had a purity of greater than 95% and an overall yield of 42% (or 40.8 mg using our synthesis scale). The peptide showed excellent analytical characteristics due to the presence of the methylcoumarin (MCA) fluorescent label. The MCA fluorophore also facilitated subsequent purification steps, owing to the ability to detect the compound. In our experience, PEG-lipid constructs without a fluorescent label have proven difficult to synthesize and purify (see Supporting Information). The MCA fluorophore was found to be essential once the targeting lipid was incorporated into an LN, as the exact mole percentage of RGD-lipid in LN could then be calculated.

Incorporation of the Targeting Lipid into LNs. The amount of RGD-lipid that was incorporated into RGD-LNs made via the postinsertion method was slightly reduced ($p < 0.05$), when compared to the amount of RGD-lipid that was initially added to the LN (Figure 2). The reason that the RGD-lipid did not fully integrate into the LN bilayer may be due to the adherence of the RGD-lipid micelles to glassware and the relatively small scale of our experiments. No significant decrease in the amount of RGD-lipid was detected for RGD-LNs made by the formulation method ($p > 0.05$). Because the formulation method was more straightforward and had good incorporation yields, it was the method of choice in subsequent experiments.

Table 1. Characterization of RGD-LNs

LN formulation	number of RGD molecules at LN surface[a]	size (nm)	HUVEC binding K_d (nM)[b,c]
nontargeted	0	102.4 ± 27.3	n/a
0.5% RGD	423	102.2 ± 32.0	2.59 ± 0.58
1% RGD	846	94.2 ± 20.7	1.98 ± 0.35
2.5% RGD	2113	128.9 ± 68.0	0.38 ± 0.07
5% RGD	4226	117.4 ± 66.0	0.59 ± 0.02

[a] This value was estimated using the assumptions that 100% of the RGD-lipid was incorporated into the LN and that 57% of the total RGD-lipid resides on the outer leaflet of the LN lipid bilayer. [b] Error is expressed as ± the standard error of the estimate from the nonlinear regression curve for binding. [c] The K_d value is expressed as the concentration of RGD-LN required to achieve half saturation of HUVEC cells and is derived from the data presented in Figure 3.

RGD-LN Characterization. The RGD-lipid was readily incorporated into LNs by the formulation method. When combined with other lipids such as DSPC, cholesterol, and a fluorescently labeled PE (Rhodamine-PE), LNs exhibiting a regular Gaussian size distribution with an average diameter of approximately 100 nm could be formed using up to 5 mol % of the RGD-lipid without obvious signs of aggregation. As summarized in Table 1, the LN particle size increased slightly, with an increase in the standard deviation (an indicator of LN aggregation) when 2.5 or 5 mol % of the RGD-lipid were included in the formulation. The apparent binding constants (expressed as K_d values) shown in Table 1 were calculated from the specific binding at 4 °C (data presented in Figure 3).

RGD-LN Binding Affinities. The apparent K_d values presented in Figure 3 decrease as the proportion of RGD-lipid is increased to 2.5 mol %. It can also be observed from the data in Figure 3A that the B_{max} values observed for the 5 mol % RGD-LNs is higher than the other formulations by 1.7-fold, which could be due to some limited aggregation of the RGD-LNs at these high contents of RGD-lipid. It is important to note that the K_d value observed in Table 1 accounts for a sum of several possible cellular processes and has been simplified here to describe the overall binding of RGD-LNs to live HUVEC cells.

Drug Retention in RGD-Targeted LNs. In some cases, it has been shown that when targeting ligands are incorporated into LNs, the permeability of the LN membrane to the drug

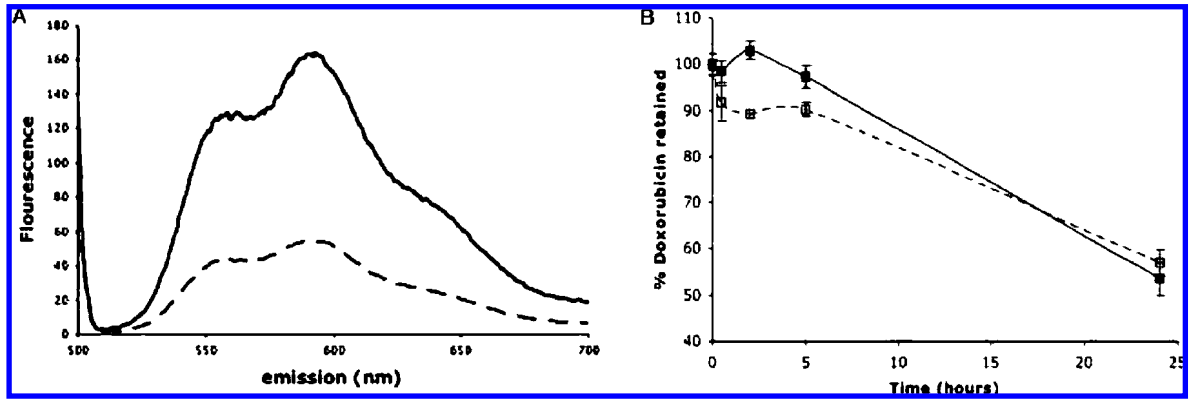

Figure 4. Doxorubicin retention in RGD-LNs versus nontargeted LNs. (A) Emission spectrum (following excitation at 490 nm) of 1.5 μg of doxorubicin dissolved in water (dashed line) or 10% Triton X-100 (solid line). (B) Release of doxorubicin from RGD-LNs made via the formulation method (solid line) and nontargeted LNs (dashed line) in a 10% FBS solution. Error is given as $\pm$ the standard deviation of three data points from the average doxorubicin emission (590 nm) determined in the presence of 10% Triton X-100.

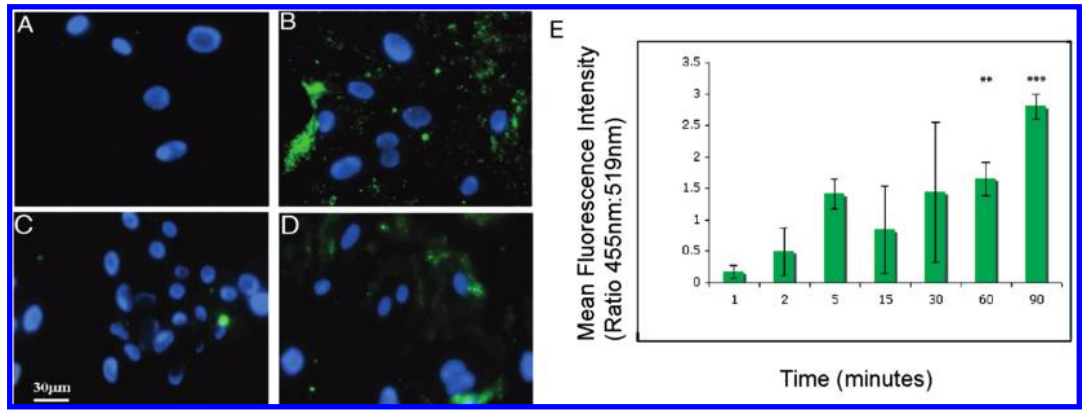

Figure 5. RGD-LNs are internalized and acidified by HUVEC. Panels A−D show fluorescence microscopy images demonstrating LN-associated HPTS uptake by HUVEC, while panel E reflects data obtained by flow cytometry which shows that the LN experiences an increasingly acidic environment as reflected by a progressive shift in the HPTS fluorescence toward fluorescence at 455 nm. LNs loaded with HPTS were coincubated with HUVEC cells at 37 °C. (A) Nontargeted LNs, 10 min incubation; (B) 1% RGD-targeted LNs, 10 min incubation. Panels C and D show HPTS:LNs that were internalized after a 40 min incubation; (C) shows the uptake of HPTS-loaded nontargeted LNs and (D) shows the 40 min uptake of 1% HPTS:RGD-LNs.

may also increase (*24*) (*25*). For this reason, the release of a commonly used anticancer drug, doxorubicin, from LN containing RGD-lipid was investigated.

Doxorubicin was loaded into LN and RGD-LN (containing 1 mol % RGD-lipid, and made by the formulation method) and the LNs were incubated in an aqueous buffer containing blood serum, over 24 h. At specified times, aliquots were withdrawn, free drug removed with a spin column, and the amount of doxorubicin remaining in the LN (upon release with Triton X-100) was assayed (Figure 4A). Little difference could be observed between the release of doxorubicin from RGD-LNs or nontargeted LNs (Figure 4B) indicating that the RGD-lipid did not significantly ($p > 0.05$) enhance the permeability of the LN membrane to doxorubicin over a 24 h period. It should be noted that the loss of nearly 30% of the LN's loaded material over 24 h is somewhat higher than that from the commercial LN formulations of doxorubicin. We attribute the relatively high loss of doxorubicin from the interior of the vesicles to the presence of serum proteins, lack of PEG coating, and incubation at physiological temperatures.

Cellular Uptake and Processing of RGD-LNs. The internalization and subsequent acidification of an RGD-LN within the cell was tracked with the pH-sensitive, membrane-impermeable probe HPTS. When HPTS is acidified, the emission spectrum shifts to shorter wavelengths. HPTS was loaded into LNs as indicated in Experimental Procedures. The LNs were then added to HUVECs and subjected to fluorescence microscopy. Green fluorescence in punctate cytoplasmic vesicles could be observed within 10 min in cells incubated with RGD-LNs, but not in cells incubated with nontargeted LNs (Figure 5A,B). The fluorescent signal detected after a 40 min incubation (Figure 5D) is noticeably more diffuse, suggesting that the fluorophore escapes the endosome at some time between 10 and 40 min following association of the RGD-LN with the HUVEC.

Figure 5E supports the notion that acidification is a function of incubation time. The fluorescence properties of HPTS were investigated with flow cytometry, using the indication of a neutral pH environment (fluorescence emission at 519 nm following excitation at 495 nm) or an acidic environment (emission at 455 nm following excitation at 405 nm). These results indicate that internalization of the particle commenced as early as 5 min. A significant increase in the relative 455 nm fluorescence was observed after 60 min suggesting that the contents within the particle are processed in a manner that coincides with endosomal maturation.

In Vitro Drug Delivery by RGD-LNs. Fluorescence microscope images comparing the delivery of doxorubicin by LNs versus the free drug are presented in Figure 6. Free, unencapsulated doxorubicin has a high affinity for the cell nucleus and rapidly permeates the plasma membrane. Thus, the fluorescence signal for free doxorubicin almost entirely colocalizes with the nuclear stain, DAPI (Figure 6A). Conversely, 1 mol % RGD-LNs deliver doxorubicin to cytoplasmic compartments (Figure 6B). Doxorubicin delivered by nontargeted LNs shows minimal

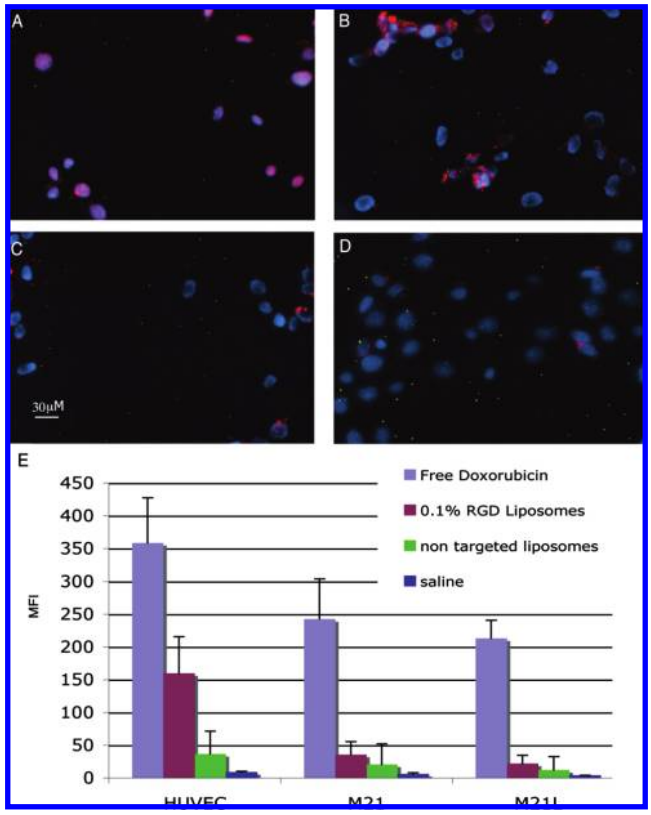

Figure 6. Cellular uptake of doxorubicin as a free drug, encapsulated in nontargeted LNs or in RGD-LNs. Panels A−D: Doxorubicin uptake by HUVEC cells as monitored by fluorescence microscopy following a 30 min incubation at 37 °C with the same amount of doxorubicin (0.265 mM) delivered to cells as (A) free drug, (B) 1% RGD-LN, (C) nontargeted LN, or (D) saline background control. (E) Doxorubicin uptake (as measured by flow cytometry) by three cell lines with different levels of $\alpha_v\beta_3$ expressed on their surface, HUVEC, M21, or M21L. 0.08 mM of doxorubicin was added to cells as either free, RGD-LN, or nontargeted LN formulations and incubated for 1 h at 37 °C prior to analysis.

background staining with uptake levels similar to the saline control (Figure 6C,D).

The ability of RGD-LNs to deliver doxorubicin to $\alpha_v\beta_3$-expressing cells is supported by the flow cytometry experiments shown in Figure 6E. HUVECs express approximately 263 000 $\alpha_v\beta_3$ integrins per cell, whereas M21 and M21L melanoma cells express approximately 56 700 and 1400 integrins per cell, respectively (*22*). RGD-LNs deliver more doxorubicin to HUVECs than nontargeted LN ($p < 0.05$) and appear to deliver modestly higher amounts to M21 cells over the nontargeted LNs; however, this increase is not statistically significant ($p > 0.05$). In contrast, M21L cells that express a relatively low amount of the receptor do not show enhanced uptake of doxorubicin-containing RGD-LNs.

DISCUSSION

This study describes well-defined RGD-lipid formulations that can target anticancer drugs to endothelial cells. Much of our ability to define the RGD-LNs used in this study is attributable to the inclusion of a defined-length, PEG-based spacer. We found that using this spacer improved upon the handling properties of the compound and facilitated analysis by ESI-MS, enabling a defined mass to confirm the identity of the compound. On several occasions, the shielding effect of PEG units was problematic toward the synthesis and purification of the construct. This was particularly important for confirmation of successful couplings while the construct was on a solid phase. In such case, robust qualitative methods (ESI-MS) were required to confirm couplings. The same concern may be raised toward the analysis of a successful purification when the construct was cleaved from the resin.

It is important to note that the PEG−lipid conjugate used in this study differs from commonly used PEG polymers, which are an average molecular weight of PEG repeats. The approximate bond length of the spacer is 75.7 Å. This estimate does not consider the bending and rotation of the spacer in aqueous solutions, which could be more accurately assessed using SPR-based techniques. Such techniques describe the extension of PEG-spacers in water. Using this methodology, it has been shown that PEG_{2000} spacers (commonly used in the manufacture of long-circulating LNs) extend approximately 200 Å from the surface of a lipid bilayer (*26*).

The ability to accurately characterize RGD-LNs is also partly attributable to the use of a fluorescent label within the RGD-lipid architecture. This was found to be essential for the accurate purification and chromatographic identification of the final product. The use of an identifying species such as a fluorescent label may lead to future preclinical targets, which may visualize and treat tumors at the same time. Indeed, RGD-conjugates to deliver imaging agents are quickly progressing through clinical trials (*27*).

Of the different methods employed to produce RGD-LNs, the formulation method was found to be the most straightforward and most effective. In our case, the post-insertion method resulted in incomplete transfer of a lipid particle between the RGD-lipid micelle and the preformed LN. It is generally thought that the post-insertion method of integrating a targeted lipid into the LN bilayer favors the orientation of the targeting lipid toward the outside layer of the LN bilayer (*28*).

A third method exists that is heavily used in the published literature on targeted LNs. This method entails reacting a targeted ligand with a functionalized group on the LN outer surface. Removal of unreacted or nonproduct species from the LN is impossible under these conditions. Furthermore, the measure of the amount of targeting ligand that ends up on the LN surface is generally unknown when using this approach.

Using defined RGD-LNs, we were able to synthesize a series of LNs that were composed of varying densities of the RGD−lipid. When the RGD-LNs were added to HUVECs, we found that an overall decrease in the observed K_d values correlated with an increase in the amount of RGD per LN. This may suggest that the improved binding of the LN can be attributed to the increased RGD valency of the LN. These findings are consistent with results published by Montet and colleagues, who found improved binding for multivalent presentations of their RGD-nanoparticles compared to their monovalent versions (*29*). In our study, we found a modest increase in K_d when the RGD−lipid is incorporated at 5 mol % versus 2.5 mol %. This small increase suggests that the optimal mole percentage of RGD−lipid per LN is within this range. It may also be possible that, after a certain concentration, there is lateral segregation of the RGD−lipid into larger aggregates. The data collected here appear to indicate that a more complex physical association is favored when RGD−lipids are incorporated at higher ratios (i.e., 2.5 and 5 mol % RGD-LNs appeared to have larger variation in particle size) to the other LN lipids. A manuscript which specifically focuses on RGD/HUVEC binding has recently been published by our group (*22*).

The major emphasis of this study is on the synthesis of a pure RGD−lipid and RGD-subsequent formulation into an RGD-LN. Our RGD−lipid is unique since it can be quantitatively formulated into LNs at the time of manufacture. The inclusion of the MCA molecule facilitated this and did not appear to affect the targeting function of the RGD−lipid. We

believe that providing good quantitative analytical data for the RGD-LN is important for *in vitro* analyses as shown in this study and will also be crucial for future *in vivo* characterization.

ACKNOWLEDGMENT

We thank Dr. David Cheresh for the melanoma cell lines, Dr. Mark Okon for NMR expertise, and Dr. Scott Covey for assistance with microscopy. Sonya Cressman is supported by funds from the National Science and Research Council. Pieter Cullis's lab is supported by grants from the Canadian Institute for Health Research and Tekmira Pharmaceuticals Inc.

Supporting Information Available: The synthesis and formulation properties of three other RGD-lipids. This material is available free of charge via the Internet at http://pubs.acs.org.

LITERATURE CITED

(1) Allen, T. M., and Chonn, A. (1987) Large unilamellar liposomes with low uptake into the reticuloendothelial system. *FEBS Lett. 223*, 42–6.

(2) Folkman, J. (1990) What is the evidence that tumors are angiogenesis dependent? *J. Natl. Cancer Inst. 82*, 4–6.

(3) Brooks, P. C., Clark, R. A., and Cheresh, D. A. (1994) Requirement of vascular integrin alpha v beta 3 for angiogenesis. *Science 264*, 569–71.

(4) Dechantsreiter, M. A., Planker, E., Matha, B., Lohof, E., Holzemann, G., Jonczyk, A., Goodman, S. L., and Kessler, H. (1999) N-Methylated cyclic RGD peptides as highly active and selective alpha(V)beta(3) integrin antagonists. *J. Med. Chem. 42*, 3033–40.

(5) Haubner, R., Gratias, R., Diefenbach, B., Goodman, S. L., Jonczyk, A., and Kessler, H. (1996) Structural and functional aspects of RGD-containing cyclic pentapeptides as highly potent and selective integrin avB3 antagonists. *J. Am. Chem. Soc. 118*, 7461–7472.

(6) Kim, J. W., and Lee, H. S. (2004) Tumor targeting by doxorubicin-RGD-4C peptide conjugate in an orthotopic mouse hepatoma model. *Int. J. Mol. Med. 14*, 529–35.

(7) Chen, X., Hou, Y., Tohme, M., Park, R., Khankaldyyan, V., Gonzales-Gomez, I., Bading, J. R., Laug, W. E., and Conti, P. S. (2004) Pegylated Arg-Gly-Asp peptide: 64Cu labeling and PET imaging of brain tumor alphavbeta3-integrin expression. *J. Nucl. Med. 45*, 1776–83.

(8) Xiong, X. B., Huang, Y., Lu, W. L., Zhang, X., Zhang, H., Nagai, T., and Zhang, Q. (2005) Intracellular delivery of doxorubicin with RGD-modified sterically stabilized liposomes for an improved antitumor efficacy: in vitro and in vivo. *J. Pharm. Sci. 94*, 1782–93.

(9) Wang, L., Shi, J., Kim, Y. S., Zhai, S., Jia, B., Zhao, H., Liu, Z., Wang, F., Chen, X., Liu, S. (2008) Improving tumor-targeting capability and pharmacokinetics of (99m)Tc-labeled cyclic RGD dimers with PEG(4) linkers. *Mol. Pharm*.

(10) Schraa, A. J., Kok, R. J., Moorlag, H. E., Bos, E. J., Proost, J. H., Meijer, D. K., de Leij, L. F., and Molema, G. (2002) Targeting of RGD-modified proteins to tumor vasculature: a pharmacokinetic and cellular distribution study. *Int. J. Cancer 102*, 469–75.

(11) Dubey, P. K., Mishra, V., Jain, S., Mahor, S., and Vyas, S. P. (2004) Liposomes modified with cyclic RGD peptide for tumor targeting. *J. Drug Targeting 12*, 257–64.

(12) Xiong, X. B., Huang, Y., Lu, W. L., Zhang, X., Zhang, H., Nagai, T., and Zhang, Q. (2005) Intracellular delivery of doxorubicin with RGD-modified sterically stabilized liposomes for an improved antitumor efficacy: in vitro and in vivo. *J. Pharm. Sci. 94*, 1782–93.

(13) Holig, P., Bach, M., Volkel, T., Nahde, T., Hoffmann, S., Muller, R., and Kontermann, R. E. (2004) Novel RGD lipopeptides for the targeting of liposomes to integrin-expressing endothelial and melanoma cells. *Protein Eng. Des. Sel. 17*, 433–41.

(14) Nabors, L. B., Mikkelsen, T., Rosenfeld, S. S., Hochberg, F., Akella, N. S., Fisher, J. D., Cloud, G. A., Zhang, Y., Carson, K., Wittemer, S. M., Colevas, A. D., and Grossman, S. A. (2007) Phase I and correlative biology study of cilengitide in patients with recurrent malignant glioma. *J. Clin. Oncol. 25*, 1651–7.

(15) Torchilin, V. (1985) Liposomes as targetable drug carriers. *Crit. Rev. Ther. Drug Carrier Syst. 2*, 65–115.

(16) Jansons, V. K., and Mallett, P. L. (1981) Targeted liposomes: a method for preparation and analysis. *Anal. Biochem. 111*, 54–9.

(17) Heath, T. D., Montgomery, J. A., Piper, J. R., and Papahadjopoulos, D. (1983) Antibody-targeted liposomes: increase in specific toxicity of methotrexate-gamma-aspartate. *Proc. Natl. Acad. Sci. U.S.A. 80*, 1377–81.

(18) Nellis, D. F., Ekstrom, D. L., Kirpotin, D. B., Zhu, J., Andersson, R., Broadt, T. L., Ouellette, T. F., Perkins, S. C., Roach, J. M., Drummond, D. C., Hong, K., Marks, J. D., Park, J. W., and Giardina, S. L. (2005) Preclinical manufacture of an anti-HER2 scFv-PEG-DSPE, liposome-inserting conjugate. 1. Gram-scale production and purification. *Biotechnol. Prog. 21*, 205–20.

(19) Nellis, D. F., Giardina, S. L., Janini, G. M., Shenoy, S. R., Marks, J. D., Tsai, R., Drummond, D. C., Hong, K., Park, J. W., Ouellette, T. F., Perkins, S. C., and Kirpotin, D. B. (2005) Preclinical manufacture of anti-HER2 liposome-inserting, scFv-PEG-lipid conjugate. 2. Conjugate micelle identity, purity, stability, and potency analysis. *Biotechnol. Prog. 21*, 221–32.

(20) Allen, T. M., Sapra, P., and Moase, E. (2002) Use of the post-insertion method for the formation of ligand-coupled liposomes. *Cell Mol. Biol. Lett. 7*, 217–9.

(21) Olson, F., Hunt, C. A., Szoka, F. C., Vail, W. J., and Papahadjopoulos, D. (1979) Preparation of liposomes of defined size distribution by extrusion through polycarbonate membranes. *Biochim. Biophys. Acta 557*, 9–23.

(22) Cressman, S., Sun, Y., Maxwell, E. J., Fang, N., Chen, D. D. Y., Cullis, P. (2009) Binding and uptake of RGD-containing ligands to cellular $\alpha v\beta 3$. *Int. J. Pept. Res. Ther. 15*.

(23) Haran, G., Cohen, R., Bar, L. K., and Barenholz, Y. (1993) Transmembrane ammonium sulfate gradient in liposomes produce efficient and stable entrapment of amphipathic weak bases. *Biochim. Biophys. Acta 1151*, 201–15.

(24) Ishida, T., Iden, D. L., and Allen, T. M. (1999) A combinatorial approach to producing sterically stabilized (Stealth) immunoliposomal drugs. *FEBS Lett. 460*, 129–33.

(25) Nallamothu, R., Wood, G. C., Kiani, M. F., Moore, B. M., Horton, F. P., and Thoma, L. A. (2006) A targeted liposome delivery system for combretastatin A4: formulation optimization through drug loading and in vitro release studies. *PDA J. Pharm. Sci. Technol. 60*, 144–55.

(26) Jeppesen, C., Wong, J. Y., Kuhl, T. L., Israelachvili, J. N., Mullah, N., Zalipsky, S., and Marques, C. M. (2001) Impact of polymer tether length on multiple ligand-receptor bond formation. *Sciences 293*, 465–8.

(27) Iagaru, A., Chen, X., and Gambhir, S. S. (2007) Molecular imaging can accelerate anti-angiogenic drug development and testing. *Nat. Clin. Pract. Oncol. 4*, 556–7.

(28) Lammers, T., Hennink, W. E., and Storm, G. (2008) Tumour-targeted nanomedicines: principles and practice. *Br. J. Cancer 99*, 392–7.

(29) Montet, X., Funovics, M., Montet-Abou, K., Weissleder, R., and Josephson, L. (2006) Multivalent effects of RGD peptides obtained by nanoparticle display. *J. Med. Chem. 49*, 6087–93.

BC900041F